

**Differential Scanning Calorimetry of Chloramphenicol Palmitate and the Phase-Transitional Behavior of Chloramphenicol Palmitate observed during the Preparation of Its Oral Suspension<sup>1)</sup>**MASATOSHI A. MIYAMOTO, TOMOAKI KIYOTAKI, NAO A. KISOH,  
TAKAYOSHI MITSUNAGA, and TADAO MAEDA*Formulation Research Department, Ibaraki Plant, Pharmaceuticals Division,  
Sumitomo Chemical Co., Ltd.<sup>2)</sup>*

(Received July 27, 1972)

Differential scanning calorimetry was carried out to elucidate the properties of two metastable forms of chloramphenicol palmitate ( $\delta$  form and sub- $\alpha$  form) and the occurrence and the role of the sub- $\alpha$  form during manufacturing of chloramphenicol palmitate oral suspension.

The  $\delta$  form, a new form, was obtained when the small amount of melted chloramphenicol palmitate was cooled very rapidly to below  $0^\circ$  and it was converted to the sub- $\alpha$  form at  $23^\circ$  on heating. The X-ray diffraction pattern of the  $\delta$  form was distinguished from that of any other forms reported. The other form, sub- $\alpha$ , was obtained by warming the  $\delta$  form or directly from the melt by rapid cooling. It was transformed to the  $\alpha$  form while liberating heat from about  $40^\circ$  through about  $75^\circ$ . The X-ray diffraction pattern, infrared absorption spectra, the behavior in the hot stage of the polarizing microscope and the differential scanning calorimetric curves suggested that the sub- $\alpha$  form is composed of the crystallites of the  $\alpha$  form. Estimated thermodynamic values at the 95% confidence limit were;  $\Delta H_{\text{melt} \rightarrow \text{sub-}\alpha} = -9.2 \pm 0.2$  kcal/mole,  $\Delta H_{\text{melt} \rightarrow \delta} = -2.8 \pm 0.5$  kcal/mole,  $\Delta H_{\delta \rightarrow \text{sub-}\alpha} = -2.2 \pm 0.7$  kcal/mole, and  $\Delta H_{\text{sub-}\alpha \rightarrow \alpha} = -2.0 \pm 0.3$  (the sub- $\alpha$  form directly from the melt) and  $-6.1 \pm 0.9$  kcal/mole (the sub- $\alpha$  form *via* the  $\delta$  form).

The supercooled dispersion of chloramphenicol palmitate in the emulsifier solution turned into the suspension while stirring. The first solid state of the chloramphenicol palmitate was estimated to be the sub- $\alpha$  form and it was transformed to the  $\alpha$ -form gradually.

The polymorphism of the long chain esters of chloramphenicol, especially palmitate, has been investigated from the physicopharmaceutical,<sup>3)</sup> biopharmaceutical,<sup>4)</sup> industrial<sup>5)</sup>

- 1) A part of this paper was presented at the 92nd Annual Meeting of Pharmaceutical Society of Japan, Osaka, Apr. 1972.
- 2) Location: *Oada-Kuwagauchi 151, Ibaraki, Osaka, 567, Japan.*
- 3) a) K. Inami, H. Takada, S. Ueda, K. Tsukada, T. Suyama, and T. Hoshi, *Takamine Kenkyusho Nempo*, **11**, 84 (1959); b) H. Negoro, S. Ueda, T. Suyama, and T. Hoshi, *ibid.*, **12**, 141 (1960); c) C. Tamura and H. Kuwano, *Yakugaku Zasshi*, **81**, 755 (1961); d) *Idem, ibid.*, **81**, 759 (1961); e) L. Borka and K. Backe-Hansen, *Acta Pharm. Suecica*, **5**, 525 (1968); f) L. Borka, *ibid.*, **7**, 1 (1970); g) *Idem, ibid.*, **8**, 365 (1971); h) A. J. Aguiar, *J. Pharm. Sci.*, **58**, 963 (1969); i) A. J. Aguiar and J.E. Zelmer, *ibid.*, **58**, 983 (1969); j) M. Hata, Dissertation for Master's Degree, Chiba University, 1969; k) Y. Nakai, "Calorimetry, Thermometry, and Thermal Analysis, 1970 Edition," ed. by the Society of Calorimetry and Thermal Analysis, Kagaku Gijitsusha, Tokyo, 1971, p. 85.

and analytical<sup>6)</sup> points of view.

Three polymorphs and one amorphous form of chloramphenicol palmitate have been reported. The  $\beta$  form (Form A) is the most stable form and bio-inactive. The  $\alpha$  form (Form B) is one of the metastable forms and bio-active. Form C was obtained by rapid quenching of the warm absolute methanol solution of chloramphenicol palmitate.<sup>3e)</sup> In this report this form will be called " $\gamma$  form."

The first publication describing the amorphous form was presented by Kimura and Hashimoto<sup>5a)</sup> who claimed a patent for the preparation method of the amorphous form by rapid quenching of the chloramphenicol palmitate solution in hydrophilic solvents. Later Tamura and Kuwano<sup>3e)</sup> reported that they obtained the amorphous form by rapid quenching of the melted chloramphenicol palmitate in the refrigerator to  $-10^\circ$ . The term "amorphous" was also used in other literatures,<sup>4a-c, 4e-g)</sup> but there are some confusions. In the extreme case X-ray diffraction data of the amorphous form were presented.<sup>4f)</sup> It seemed to us that the term "amorphous" was used microscopically in some cases and X-ray diffractometrically in other cases.

In the present report the term "amorphous form" was excluded for its ambiguity. Instead, the concepts of two less stable forms were adopted, *i.e.* the sub- $\alpha$  form and the  $\delta$  form. Their definitions and interpretations will be described in "Result and Discussion."

Borka compared the thermal behavior of the four reported forms and could not find any differences among the  $\alpha$  form, the  $\gamma$  form and the so-called amorphous form by differential scanning calorimetry.<sup>3f)</sup> The first purpose of the present investigation was to compare the thermal behaviors of the reported polymorphs.

The second purpose was to check the possibility of existence of a new phase,  $\delta$  form, suggested by a small exothermic peak at  $23^\circ$  on heating after rapid quenching of the melt in differential scanning calorimetry.

The last purpose was to elucidate the mechanism of the crystallization of chloramphenicol palmitate during the manufacturing of chloramphenicol palmitate oral suspension.

In the following parts differential scanning calorimetry will be called calorimetry and the differential scanning calorimeter will be abbreviated as DSC.

### Experimental

Two grades of chloramphenicol palmitate were used. The pure compound was synthesized from chloramphenicol J.P. and 99.5% pure palmitoyl chloride according to a Hungarian patent<sup>7)</sup> and recrystallized from methanol-water and toluene-hexane five times each. After the purification any impurities were not detected by thin-layer chromatography. Also chloramphenicol palmitate J.P. was used for the preparation of the oral suspension and for X-ray diffractometry.

- 4) a) L. Almirante, I. De Carneri, and G. Coppi, *Farmaco Ed. Prat.*, **15**, 471 (1960); b) J. Dony and A. De Roeck, *J. Pharm. Belg.*, **20**, 475 (1965); c) C.M. Anderson, *Austral. J. Pharm.*, **47**, S44 (1966); d) A.J. Aguiar, J. Krc, Jr., A.W. Kinkel, and J.C. Samyn, *J. Pharm. Sci.*, **56**, 847 (1967); e) L. Coclers, *Acta Pharm. Jugoslav.*, **17**, 141 (1967); f) E. Goeres, H.G. Walther, U. Steinike, A. Wehl, and R. Beise, *Deut. Gesundheitswesen*, **23**, 306 (1968); g) A.J. Aguiar, *Drug Information Bulletin*, **3**, 17 (1969); h) S. Banerjee, A. Bandyopadhyay, R. C. Bhattacharjee, A.K. Mukherjee, and A.K. Halder, *J. Pharm. Sci.*, **60**, 153 (1971).
- 5) a) T. Kimura and S. Hashimoto, Japan. Patent 60-5798 (1960); b) H.G. Walther, E. Goeres, and K. Berendt, Ger. (East) Patent 54685 (1967); c) S. Kawamura, T. Hirano, S. Takamura, and M. Okazaki, Ger. Patent 1936176 (1970); d) E. Akito, T. Takagi, Y. Aoda, and M. Ishibashi, Ger. Patent 2015263 (1970); e) Y. Ueda, H. Fujii, S. Furuyama, and M. Tanino, Japan. Patent 70-33199 (1970); f) R. Okada, Japan. Patent 71-16969 (1971); g) R. Okada and T. Suyama, Japan. Patent 71-26985 (1971).
- 6) a) M. Maruyama, N. Hayashi, and M. Kishi, *Takamine Kenkyusho Nempo*, **13**, 176 (1961); b) H. Kuwano and C. Tamura, *Yakugaku Zasshi*, **81**, 764 (1961); c) L. Borka and K. Backe-Hansen, *Acta Pharm. Suecica*, **5**, 271 (1968).
- 7) L. Levai and P. Szekeley, Hungarian Patent 150032 (1963).

The well-maintained Perkin-Elmer DSC 1B modified to be able to scan at  $0.156^\circ/\text{min}$  and  $0.313^\circ/\text{min}$  in addition to the normal scanning velocities was used for calorimetry. Temperature calibration was carried out with 99.999% pure indium daily and with some organic compounds when necessary. The area under the peak was measured planimetrically. The weight of the specimen for calorimetry was around 1 mg and measured with Shimadzu Electric Balance PMC-50.

The photographs of X-ray diffraction pattern were taken with Nonius Weissenberg Camera Y809, 57.3 mm in diameter, and Toshiba X-Ray Generator ADP-301. The low-temperature device kept the specimen at  $-5^\circ$  during measurement. The diffraction diagram of the photographs was recorded with Shimadzu PD-20 Densitometer. Also Rigaku Denki Geiger Flex D-2 was used for the identification of the  $\gamma$  form and for the oral suspension study.

Infrared spectra were taken with Hitachi EPI-G Type Infrared Spectrophotometer.

The observation with crossed polars was undertaken using a polarizing microscope<sup>8)</sup> with a hot stage.<sup>9)</sup> The temperature indication of the hot stage was calibrated by measuring melting points of azobenzene, chloramphenicol palmitate ( $\beta$  form) and acetophenone.

The oral suspension was prepared as follows. One hundred and nine grams of chloramphenicol palmitate J.P. alone was melted at around  $95^\circ$ , added into a solution prepared by dissolving 40 g of polyvinyl alcohol in 900 ml of water heated at  $90-95^\circ$  and mixed by a suitable agitator. The mixture was quenched to  $30^\circ$  in an ice bath. After adding 15 g of surface active agents dissolved in 100 ml of water, the cooled dispersion was warmed and kept at  $40^\circ$  while stirring. No other components used for usual production were added in this experiment. The samples for X-ray diffractometry, for calorimetry and for microscopy were drawn out from the dispersion and the torque of the stirrer was recorded at adequate intervals. The particle size of the final product was determined by sedimentation analysis using Micron Photo Sizer Model MSR (Seiko Boeki Co., Ltd.) after adequate dilution.

## Result and Discussion

### Detection of the $\beta$ Form

A melt-mediated transition from the  $\alpha$  form of chloramphenicol palmitate to the  $\beta$  form on heating was reported.<sup>3k)</sup> As this transition was thought to be due to the presence of the nuclei of the  $\beta$  form, this phenomenon was applied to the detection of a small amount of the  $\beta$  form. The specimen was heated to the melting point of the  $\alpha$  form in the DSC and cooled to a room temperature. The specimen was heated again to  $100^\circ$ . Although the freshly prepared  $\alpha$  form in the DSC remained  $\alpha$  after the treatment above, the sample containing even a small amount of the  $\beta$  form turned into the  $\beta$  form. The sensitivity was much higher than the infrared absorption method<sup>6a)</sup> and the X-ray diffraction method.<sup>6b)</sup> The details of this method and the application to the preparation will be described in the following paper.

### Differential Scanning Calorimetry

Although temperature calibration of the DCS was conducted before and after the experiment daily, the temperature indication of the DSC is not thought to express the true temperature of a sample correctly. The temperature values appear in the following parts should not be regarded as exact temperatures.

The thermograms of chloramphenicol palmitate during one cooling-heating cycle from  $100^\circ$  to  $100^\circ$  *via*  $-10^\circ$  were classified into three types. Fig. 1 illustrates these three patterns and

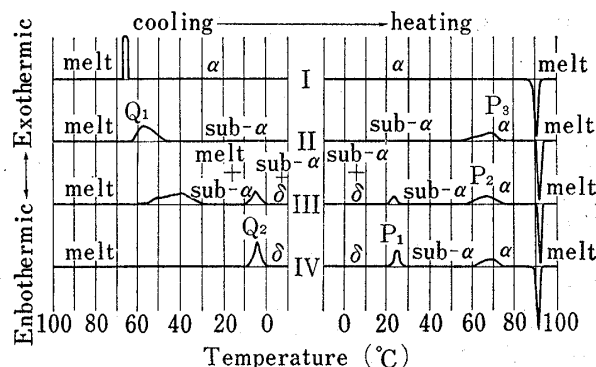


Fig. 1. Schematic Differential Scanning Calorimetric Thermograms of Pure Chloramphenicol Palmitate

cooling rate: I,  $0.156-0.625^\circ/\text{min}$ ; II,  $1.25-10^\circ/\text{min}$ ; III,  $20-40^\circ/\text{min}$ ; IV, ideal rapid quenching; heating rate:  $5^\circ/\text{min}$  Relative magnitude of the peak areas is not exactly shown.

8) Nihon Kogaku POH-2.

9) Union MHS.

TABLE I. Summary of the Values of Enthalpy Changes

Pattern	Cooling rate (°/min)	Peak	Exo. or endo.	Sample size	$\Delta H^a$ (kcal/mole)	Standard deviation (kcal/mole)	Transition
I	0.625	$Q_1$	exo.	7	$-10.8 \pm 0.5$	0.52	melt $\rightarrow$ $\alpha$
		$P_3$	endo.	7	$10.9 \pm 0.3$	0.30	$\alpha \rightarrow$ melt
II	10	$Q_1$	exo.	11	$-9.2 \pm 0.2$	0.26	melt $\rightarrow$ sub- $\alpha$
		$P_2$	exo.	11	$-2.0 \pm 0.3$	0.41	sub- $\alpha \rightarrow$ $\alpha$
		$P_3$	endo.	11	$11.0 \pm 0.3$	0.36	$\alpha \rightarrow$ melt
		$Q_1 + P_2$	exo.	11	$-11.2 \pm 0.3$	0.48	melt $\rightarrow$ $\alpha^b$
		$Q_1 + P_3$	endo.	11	$1.8 \pm 0.3$	0.42	$\alpha \rightarrow$ sub- $\alpha^b$
III	40	$P_3$	endo.	10	$11.1 \pm 0.3$	0.41	$\alpha \rightarrow$ melt
		$Q_1 + Q_2$ $+ P_1 + P_2$	exo.	5	$-10.7 \pm 0.5$	0.38	melt $\rightarrow$ $\alpha^b$
IV	Ideally rapid	$Q_2^c$	exo.	—	$-2.8 \pm 0.5$	—	melt $\rightarrow$ $\delta$
		$P_1^c$	exo.	—	$-2.2 \pm 0.7$	—	$\delta \rightarrow$ sub- $\alpha$
		$P_2^c$	exo.	—	$-6.1 \pm 0.9$	—	sub- $\alpha \rightarrow$ $\alpha$

a) The 95% confidence limits of the average value were estimated using *t*-test. No significant differences were observed among the values of  $P_3$  of Patterns I, II and III and between the following pairs of the absolute average values at the 5% level of significance:  $Q_1$  and  $P_3$  of I,  $Q_1 + P_2$  and  $P_3$  of II,  $Q_1 + P_3$  and  $P_2$  of II, and  $Q_1 + Q_2 + P_1 + P_2$  and  $P_3$  of III. Very highly significant differences were found between the values of  $Q_1$  of I and II and between the absolute values of  $P_3$  and  $Q_1$  of II at the 0.1% level of significance. The homogeneity of the variances was confirmed using *F*-test at the 5% level of significance before testing the difference of the average values.

b) The intermediate transition or transitions were not written.

c) Estimated using equations (1), (2) and (5).

one imaginary pattern. The values of the enthalpy change were statistically treated and summarized in Table I. The significance of the differences between average values was tested at the 5% level unless otherwise noted and the 95% confidence limits of the average value were estimated.

Pattern I was found at the cooling velocities ranging from 0.156°/min through 0.625°/min. In these cases only one exothermic peak  $Q_1$  on cooling corresponding to the crystallization of the melt to the  $\alpha$  form and one endothermic peak  $P_3$  on heating corresponding to the fusion of the  $\alpha$  form were found. No crystallization to the  $\beta$  form occurred even on the slowest cooling.<sup>10)</sup>

The enthalpy changes  $\Delta H_{melt \rightarrow \alpha}$  ( $Q_1$ ) and  $\Delta H_{\alpha \rightarrow melt}$  ( $P_3$ ) were essentially the same values with opposite signs,  $-10.8 \pm 0.5$  kcal/mole and  $10.9 \pm 0.3$  kcal/mole, respectively.

Pattern II was observed when the cooling velocities were ranging from 1.25°/min through 10°/min. Fig. 2 shows a typical example of the thermogram of this pattern. In this pattern the  $Q_1$  value was significantly less than that of Pattern I at the 0.1% level of significance and was  $-9.2 \pm 0.2$  kcal/mole. Also a very highly significant difference was found between the absolute values of  $Q_1$  and  $P_3$  ( $11.0 \pm 0.3$  kcal/mole). An exothermic peak  $P_2$  appeared on the heating curve. This peak was very broad ranging from about 40° to about 75° and the value was  $-2.0 \pm 0.3$  kcal/mole. No significant differences were found between the absolute values of  $P_2$  and  $P_3 + Q_1$  and between the absolute values of  $P_3$  and  $Q_1 + P_2$ . We named the solid state of the chloramphenicol palmitate with  $P_2$  on heating "sub- $\alpha$  form."

Preliminary runs showed that  $P_2$  occurred irreversibly. A specimen of the sub- $\alpha$  form was heated up to 61° (in the middle of  $P_2$ ) and immediately cooled to 31° manually. Then the specimen was heated again until it melted and  $P_2$  began from about 47° and not from 61°. This result shows that the change corresponding to  $P_2$  depended not only on the temperature but also on the time. The part of  $P_2$  up to 61° of the first heating corresponded to  $-0.7$

10) When 10 mg of the specimen was used, crystallization to the  $\beta$  form was observed once out of five runs at the cooling velocity of 0.156°/min.

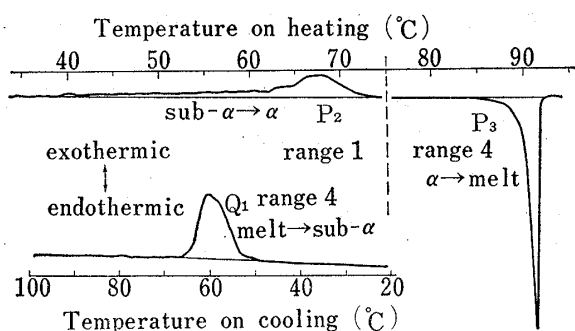


Fig. 2. Typical Cooling and Heating Curves of Pattern II

lower: cooling curve (100°→-10°, 10°/min); upper: heating curve (-10°→100°, 5°/min) The broken line shows that the range was changed.

exotherms:  $Q_1$  9.2    endotherm:  $P_3$  10.8 kcal/mole  
 $P_2$  2.0  
 total 11.2 kcal/mole

The height of the  $P_2$  peak was drawn four times larger than that of the other peaks by changing the range of the recorder.

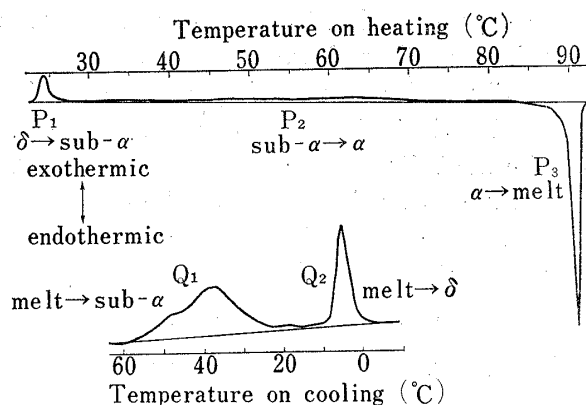


Fig. 3. Typical Cooling and Heating Curves of Pattern III

lower: cooling curve (127° → -10°, 40°/min); upper: heating curve (-10° → 127°, 5°/min)

exotherms:  $Q_1$  3.8    endotherm:  $P_3$  10.4 kcal/mole  
 $Q_2$  1.7  
 $P_1$  1.3  
 $P_2$  4.0  
 total 10.8 kcal/mole

kcal/mole and the  $P_2$  value of the second heating was  $-1.2$  kcal/mole. The total value of  $-1.9$  kcal/mole was thought to coincide with the normal  $P_2$  value,  $-2.0 \pm 0.3$  kcal/mole.

In the third case, Pattern III, in which the cooling velocities were ranging from 20°/min through 40°/min, a new exothermic peak  $Q_2$  was found on cooling and another exothermic peak  $P_1$  on heating at 23°. Fig. 3 shows a typical example of this pattern. We named this phase with  $P_1$  "δ form." The individual values of the exothermic peaks,  $Q_1$ ,  $Q_2$ ,  $P_1$  and  $P_2$ , were scattered at repeated runs in the case of Pattern III, but the total value ( $-10.7 \pm 0.5$  kcal/mole) was reproducible and in accord with the value of the endothermic peak,  $P_3$  ( $11.1 \pm 0.3$  kcal/mole), the heat of fusion of the  $\alpha$  form. The following discussion of the  $\delta$  form was based on the data of the experiments at the cooling velocity of 40°/min. Fig. 4 shows the relationship between the values of  $P_1$  and  $Q_2$ . A straight line passing the original at the 5% level of significance was obtained using the least squares method and the proportionality between  $P_1$  and  $Q_2$  suggested that  $Q_2$  was the heat of transition from the sub- $\alpha$  form or the

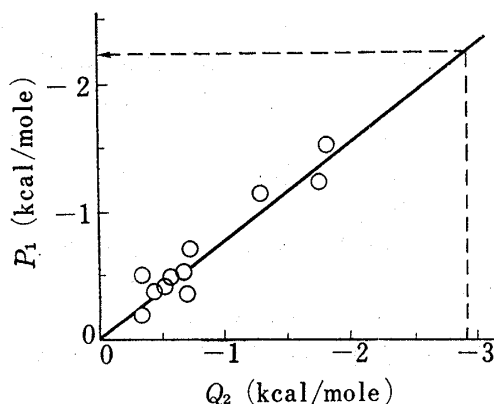


Fig. 4. Correlation between  $P_1$  and  $Q_2$  of Pattern III

cooling rate: 40°/min; heating rate 5°/min  
 The solid line,  $P_1 = 0.76Q_2$ , was obtained by the least squares method. The broken lines with an arrow indicate the extrapolation of the  $P_1$  value of the pure  $\delta$  form

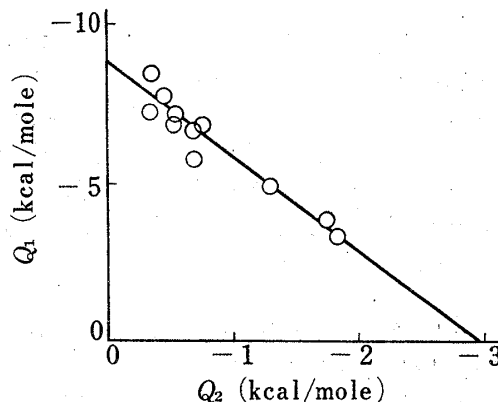


Fig. 5. Correlation between  $Q_1$  and  $Q_2$  of Pattern III

cooling rate: 40°/min; heating rate: 5°/min  
 The straight line,  $Q_1 = -3.0Q_2 - 8.7$ , was obtained by the least squares method.

heat of crystallization to the  $\delta$  form as  $P_1$  was thought to be the heat of transition from the  $\delta$  form into another phase.

In Fig. 5 the values of  $Q_1$  were plotted against the values of  $Q_2$ , where the value of  $Q_1$  decreased with the increase of the value of  $Q_2$ . This fact suggests that the  $\delta$  form was formed from the melt directly and not through the sub- $\alpha$  form.

If we express the values of the enthalpy changes of  $Q_1$ ,  $Q_2$ ,  $P_1$ ,  $P_2$  and  $P_3$  as  $Q_1$ ,  $Q_2$ ,  $P_1$ ,  $P_2$  and  $P_3$ , the expression (1) can be written as the total heat change should be zero in the cycle; melt at  $100^\circ \rightarrow$  solid at  $-10^\circ \rightarrow$  melt at  $100^\circ$ .

$$Q_1 + Q_2 + P_1 + P_2 + P_3 = 0 \quad (1)$$

From Fig. 4, the relation (2) was obtained.

$$P_1 = 0.76Q_2 \quad (2)^{11)}$$

As we did not know whether the  $\delta$  form turned into the sub- $\alpha$  form or into the  $\alpha$  form or else at  $P_1$ , it was postulated that the  $\delta$  form turned into the sub- $\alpha$  form. Then  $P_2$  was assumed to be composed of two contributions from the enthalpy change due to the transition from the sub- $\alpha$  form, which solidified from the melt directly at  $Q_1$ , to the  $\alpha$  form and from the enthalpy change due to the transition from the sub- $\alpha$  form, which was produced through the  $\delta$  form, to the  $\alpha$  form. The first contribution may be written as  $mQ_1$ , where  $m$  is a positive constant, for  $Q_1$  should be proportional to the amount of the sub- $\alpha$  form directly from the melt. On the other hand, the second contribution may be expressed as  $nQ_2$ , where  $n$  is a constant, since  $Q_2$  should be proportional to the amount of the sub- $\alpha$  form *via* the  $\delta$  form. Then the expression (3) could be written as follows.

$$P_2 = mQ_1 + nQ_2 \quad (3)$$

If the  $\delta$  form turned into the  $\alpha$  form at  $P_1$ ,  $n$  would be zero.

Introducing (2) and (3) into (1), eq. (4) was obtained.

$$Q_1 = -(1.76+n)Q_2/(1+m) - P_3/(1+m) \quad (4)$$

Eq. (4) shows the linear correlation between the values of  $Q_1$  and  $Q_2$  as  $P_3$  was constant. From Fig. 5 the relationship,

$$Q_1 = -2.9Q_2 - 8.6, \quad (5)^{12)}$$

was obtained. As  $P_3$  was  $11.1 \pm 0.3$ , the comparison between eqs. (4) and (5) gave the results that  $m$  was  $0.29 \pm 0.11$  and that  $n$  was  $2.0 \pm 0.9$  (95% confidence limits). The result that  $n$  was not zero means that the  $\delta$  form was transformed into the sub- $\alpha$  form at  $23^\circ$  on heating *i.e.* at  $P_1$ .

The cooling velocity of  $40^\circ/\text{min}$  might surpass in part the rates of nucleation of the sub- $\alpha$  form and of growth of the nucleus and the lowest-temperature form (under the experimental conditions),  $\delta$ , crystallized from the supercooled melt. Pattern III in Fig. 1 was thought to represent the thermal behavior of the mixture of the  $\delta$  form and the sub- $\alpha$  form.

These results indicated that the thermal behavior of the pure  $\delta$  form could be illustrated as Pattern IV in Fig. 1. Then the calculation of the enthalpy changes of the pure  $\delta$  form were carried out. Using  $Q_1=0$  and  $P_3=11.1$  kcal/mole,  $Q_2=\Delta H_{\text{melt} \rightarrow \delta} = -2.8$  kcal/mole,  $P_1=\Delta H_{\delta \rightarrow \text{sub-}\alpha} = -2.2$  kcal/mole and  $P_2=\Delta H_{\text{sub-}\alpha \rightarrow \alpha} = -6.1$  kcal/mole were obtained from eq. (5), (2) and (1), respectively. The 95% confidence limits of these estimated values were calculated and shown in Table I.

The specimen in each pattern could be said to be the  $\alpha$  form just before the fusion because no significant differences were found among the values of  $P_3$  of Patterns I, II and III.

11) The slope was significant at the 0.1% level of significance and the 95% confidence limit was  $\pm 0.17$ .

12) The slope and the intercept were significant at the 0.1% level of significance. The 95% confidence limits of the slope and the intercept were  $\pm 0.7$  and  $\pm 0.7$ , respectively.

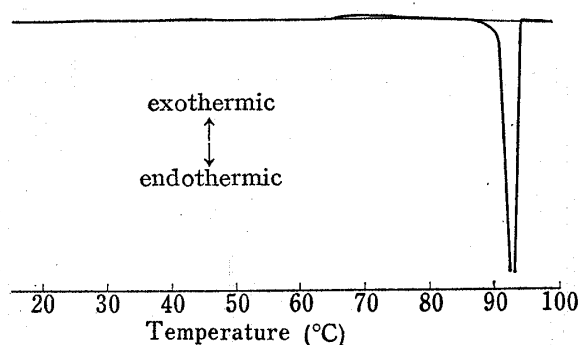


Fig. 6. Heating Curve of the  $\gamma$  Form (Form C)

heating rate:  $5^\circ/\text{min}$

The heating curve of the  $\gamma$  form is shown in Fig. 6. The  $\gamma$  form was prepared by the method of Aguiar, *et al.*<sup>36)</sup> and identified by X-ray diffractometry. A broad exothermic peak was found between about  $65^\circ$  and about  $75^\circ$  which resembled the  $P_2$  peak of the sub- $\alpha$  form although the temperature range was a little higher than that of  $P_2$  and then the  $\gamma$  form was converted to the  $\alpha$  form. The transformation from the  $\gamma$  form to the  $\alpha$  form was checked by X-ray diffractometry. No further experiments on the  $\gamma$  form were carried out.

### X-Ray Diffractometry

The specimen of the  $\delta$  form for X-ray diffractometry was prepared as follows. A glass capillary tube filled with chloramphenicol palmitate was heated in boiling water. The chloramphenicol palmitate in the capillary tube was melted and then the tube was quenched in the liquid nitrogen bath. For the identification of the phase produced, the tube containing chloramphenicol palmitate was put in a volatile sample pan and the calorimetry was run. The phase was proved to contain the  $\delta$  form.

The  $\delta$  form of the pure chloramphenicol palmitate was so unstable that at the end of the operation the transparent  $\delta$  form had already turned into the opaque sub- $\alpha$  form. This instability of the  $\delta$  form forced us to use the less purified chloramphenicol palmitate, *i.e.*, chloramphenicol palmitate J.P. for X-ray diffractometry. The  $\delta$  form of the chloramphenicol palmitate J.P. was a little more stable than that of the pure one and was intact during the diffraction measurement.

The X-ray diffraction patterns are shown in Fig. 7. The lowest curve was obtained from the diffraction diagram of the freshly quenched specimen at  $-5^\circ$ . The middle curve was obtained from the same specimen after the low-temperature controlling attachments were removed. The upper curve was obtained from the specimen after it was warmed to  $70^\circ$ . These curves were assigned to the  $\delta$  form, the sub- $\alpha$  form and the  $\alpha$  form, respectively. The weakness of the diffraction intensities will be discussed later.

### Microscopy with Crossed Polars

Some polarized photomicrographs are shown in Fig. 8. The specimen was prepared from the pure compound as that X-ray diffractometry and observed in the microscope hot stage in polarized light. As described before, the quenched specimen in a glass capillary was proved to contain the  $\delta$  form calorimetrically. But the specimen was amorphous polarizing-microscopically and on heating no visible changes were observed between about  $13^\circ$  and

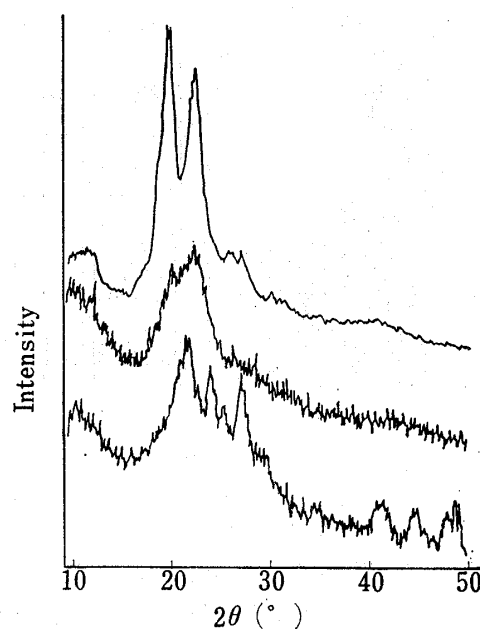


Fig. 7. X-Ray Diffraction Patterns of the  $\delta$  Form, of the Sub- $\alpha$  Form and of the  $\alpha$  Form

lower: the  $\delta$  form; middle: the sub- $\alpha$  form; upper: the  $\alpha$  form.

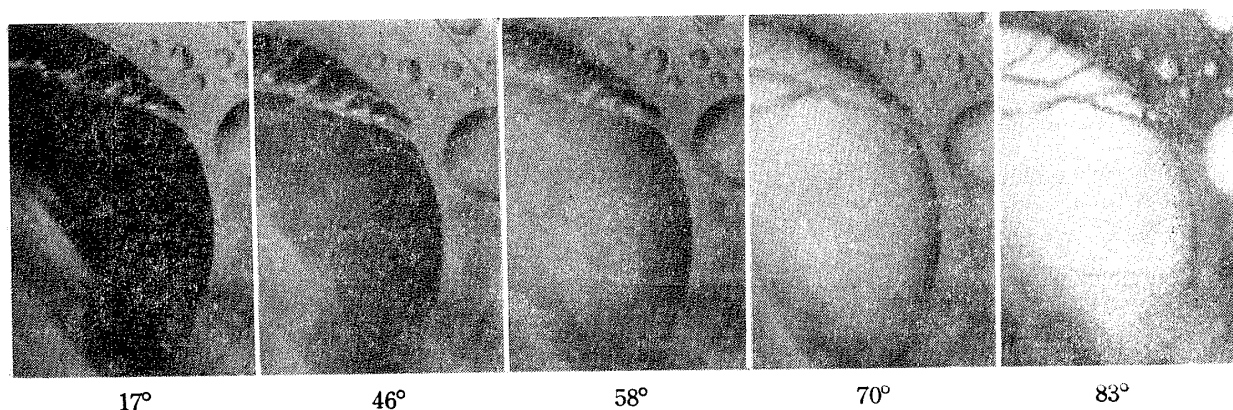


Fig. 8. Photomicrographs of the Quenched Chloramphenicol Palmitate in Polarized Light on Heating  
The photographs were taken in the same field at  $\times 40$  and the length of the shorter side of the photographs corresponds 0.5 mm.

about  $40^\circ$  although the cracks on the surface shown in the photographs in Fig. 8 indicated that the chloramphenicol palmitate was in a solid state. Over about  $45^\circ$  the chloramphenicol palmitate began to glow. Between about  $60^\circ$  and about  $70^\circ$  the change was prominent and innumerable small crystals were recognized. These small crystals melted at the melting point of the  $\alpha$  form. It is frequently experienced that the small crystals look like amorphous in polarized light. The initial amorphous appearance of the specimen might be ascribed to the smallness of the crystals. The increase of glow was estimated to correspond to the  $P_2$  peak in the calorimetry.

In another experiment the sub- $\alpha$  form on a slide glass was contacted with the  $\alpha$  form. Observation at the junction on heating indicated that the  $\alpha$  form did not grow through the particle of the sub- $\alpha$  form and that the sub- $\alpha$  form continued to grow by itself without boundary movement. This fact suggests that the both forms were the same phase.

### Infrared Spectroscopy

The infrared spectroscopy of the  $\delta$  form and the sub- $\alpha$  form was attempted but in the case of the  $\delta$  form the trial failed through its instability. The specimen of the sub- $\alpha$  form was prepared in the following manner to avoid any transformations by mulling with Nujol. The paste of chloramphenicol palmitate with Nujol was warmed to melt to about  $100^\circ$ , then cooled rapidly. The cooled mixture was examined with DSC and the chloramphenicol palmitate was identified to be the sub- $\alpha$  form. The mixture was sandwiched with sodium chloride plates and the spectra were measured as usual. The infrared spectra of the sub- $\alpha$  form and of the  $\alpha$  form were essentially identical.

### The Relation between the Sub- $\alpha$ Form and the $\alpha$ Form

The following articles were derived from the above-mentioned results of the experiments.

1. The temperatures of initiating crystallization from the melt to the sub- $\alpha$  form and to the  $\alpha$  form were essentially the same.
2. The  $Q_2$  peak in Fig. 3 shows that the crystallization from the melt to the sub- $\alpha$  form occurred between about  $60^\circ$  and about  $20^\circ$  and that the maximum was around  $40^\circ$ . This fact indicates that the supercooled melt can crystallize to the sub- $\alpha$  form at  $40^\circ$ . The  $Q_2$  peak in Fig. 2 was between about  $65^\circ$  and about  $50^\circ$ . The temperature delay of the crystallization of indium was about  $4^\circ$  between the cooling velocities of  $10^\circ/\text{min}$  and  $40^\circ/\text{min}$ . Even if considering this temperature delay, Fig. 2 suggests that all the melt had already turned into the sub- $\alpha$  form before  $40^\circ$ , otherwise the remained melt would crystallize to the  $\delta$  form below about  $20^\circ$ . In other words there was little possibility that the sub- $\alpha$  form contained the supercooled melt.



3. The X-ray diffraction pattern of the sub- $\alpha$  form shows very broad peaks whose positions were similar to those of the  $\alpha$  form although the intensities were very weak. It is generally accepted that three major factors diminish the intensities of diffraction of a crystal. The first is the crystal content in the solid. If the proportionality between the diffraction intensity and the crystal content is simply assumed, it is little possible that the sub- $\alpha$  form contained a supercooled melt for the intensity ratio of the sub- $\alpha$  form and the  $\alpha$  form was much less than the ratio of the values of  $Q_1$  of Patterns II and I. Secondly the smaller is the crystal size, the weaker is the intensity and the broader is the peak. If the crystal was very small, it gives an amorphous diffraction pattern. This phenomenon could explain our results without inconsistency. And the stronger intensity of the  $\delta$  form than that of the sub- $\alpha$  form might be attributed to the size reduction accompanying the phase transition from the  $\delta$  form to the sub- $\alpha$  form. At present no discussion can be made about the third factor, the scattering power of crystals.

4. The infrared spectra of the sub- $\alpha$  form and of the  $\alpha$  form were essentially identical.

5. The microscopy in polarized light showed small crystals of the  $\alpha$  form grew from the sub- $\alpha$  form, which was corresponding to the irreversible exothermic peak  $P_2$  of the heating curve. No boundary movement at the junction of the particles of the sub- $\alpha$  form and the  $\alpha$  form on heating was observed.

From the summary of the results it was natural to conclude that the sub- $\alpha$  form is the very small crystallites of the  $\alpha$  form and that the dimension of these crystallites may not be far from the critical dimension of the nuclei of the  $\alpha$  form. And the peak  $P_2$  showed the release of the excess energy due to the decrease of the interfacial energy and/or the strain energy among these crystallites during the growth of the crystallites of the sub- $\alpha$  form to the crystals of the  $\alpha$  form.

The discrepancy of the  $P_2$  values of the sub- $\alpha$  form directly from the melt ( $-2.0$  kcal/mole) and of that *via* the  $\delta$  form ( $-6.1$  kcal/mole) would be ascribed to the difference in the grain sizes of the sub- $\alpha$  forms. The crystallites of the sub- $\alpha$  form *via* the  $\delta$  form would be three times lesser than those of the sub- $\alpha$  form directly from the melt.

### Crystallization of Chloramphenicol Palmitate during Preparation of the Oral Suspension

In the present investigation the observation of the crystallization of chloramphenicol palmitate of the oral suspension was carried out before the sucrose syrup was added. For convenience we should like to call the oral suspension before adding sucrose "pre-syrup."

The supercooled dispersion of the pre-syrup was stirred at  $40^\circ$ . Fig. 9 shows the changes in the torque encountered during stirring the pre-syrup and the relative heat of melting of the  $\alpha$  form of chloramphenicol palmitate.

The viscosity of the pre-syrup expressed as the torque increased abruptly after about one hour and after passing maximum value decreased gradually.

The calorimetry was run with the pre-syrup sample sealed in a volatile sample pan. The reference pan was filled with the pre-syrup excluding chloramphenicol palmitate. The ratio of the heat of melting of the specimen at an arbitrary time and that of the last specimen after

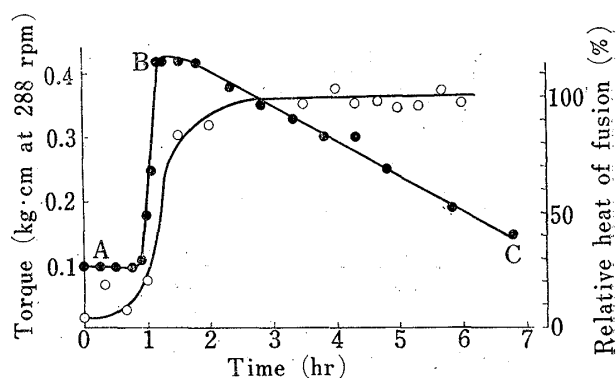


Fig. 9. Change of the Torque and the Relative Heat of Fusion of the Pre-Syrup while Maturing

Letters A, B and C represent the specimens before, at and after the maximum value of the torque.

●:torque ○:relative heat of fusion

24 hr was plotted against time in Fig. 9. This ratio was considered to express the degree of crystallization.

Comparing the both curves in Fig. 9, it was estimated the increase in viscosity was caused by the crystallization of chloramphenicol palmitate. For convenience of the further discussion three points were chosen and named A, B and C as shown in Fig. 9.

Sample A was taken immediately after the temperature of the pre-syrup reached 40°, when most of the chloramphenicol palmitate was supercooled melt though a few large dispersed particles crystallized.

Sample B was taken when the torque value reached maximum. The calorimetric data showed most of the chloramphenicol palmitate crystallized. In the polarized light the specimen looked like brilliant white clouds but the individual particles were too small to recognize.

Sample C was taken after 8 hr when the viscosity returned to the original value. Microscopic observation showed a lot of small needles growing from the white clouds. The particle size of the needles was estimated between 0.1 and 0.2  $\mu$  from the sedimentation study.

It is generally known that the smaller the particle size, the higher is the viscosity of a suspension. Considering the phenomenon, the decrease in the viscosity in this case was ascribed to the growth of the particles of the chloramphenicol palmitate.

As we discussed before, the sub- $\alpha$  form was estimated to be small crystallites of the  $\alpha$  form. In the oral suspension production the white cloud-like solid phase might be the sub- $\alpha$  form. In order to examine the white cloud-like solid phase the solid in the pre-syrup was collected by centrifugation at 10000 rpm at 20° and its X-ray diffraction pattern and thermal behavior were examined.

The X-ray diffraction patterns are shown in Fig. 10 and the heating curves corresponding to the temperature ranges characteristic of the sub- $\alpha$  form in Fig. 11. In Fig. 11 the melting behaviors of the  $\alpha$  form were omitted.

In Fig. 10 the intensity of Sample B was weakest. The reason why Sample A showed stronger intensity than Sample B will be explained as follows. The solid portion of Sample A collected was very little. This means most of the chloramphenicol palmitate was still

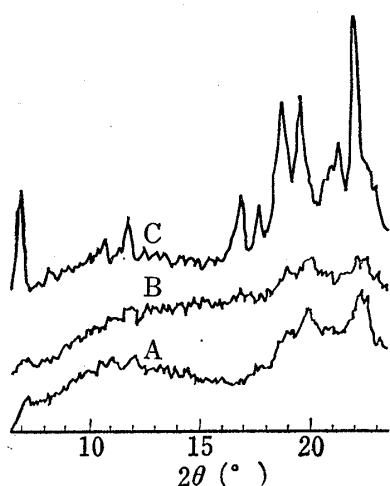


Fig. 10. X-Ray Diffraction Patterns of the Chloramphenicol Palmitate collected by Centrifugation from the Pre-Syrup

Centrifuged at 10000 rpm for 30 min at 20°; Letters A, B and C are corresponding to those in Fig. 9.

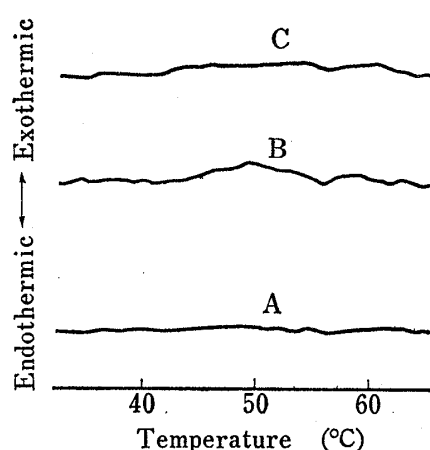


Fig. 11. Heating Curves of the Chloramphenicol Palmitate collected by Centrifugation from the Pre-Syrup

Centrifuged at 10000 rpm for 30 min at 20°, heating rate: 5°/min. All specimens had the endothermic melting peak of the  $\alpha$  form though not shown in the figure. Letters A, B and C are corresponding to those in Fig. 9.

melted. The solid might come from the large particles already crystallized to the  $\alpha$  form. On the contrary Sample B crystallized already to the small solid particles and was very difficult to centrifuge. The heating curve of the collected Sample B in Fig. 11 shows the biggest exothermal peak  $P_2$ . Both X-ray diffraction pattern and heating curve of Sample C show the chloramphenicol palmitate was converted to the  $\alpha$  form.

The summary of the results of the suspension study shows the white cloud-like solid phase of Sample B was the sub- $\alpha$  form.

1. The abrupt increase of the viscosity of the pre-syrup.
2. The white cloud-like solid in polarized light.
3. The X-ray diffraction pattern was weak but resembled that of the  $\alpha$  form.
4. The heating curve showed the exothermic peak characteristic of the sub- $\alpha$  form.

**Acknowledgement** The authors thank Mr. Masao Minobe of the Central Research Laboratory of Sumitomo Chemical Co., Ltd. for his kind help in X-ray diffractometry.